

## $\eta$ and $\eta'$ Physics at MAMI

Marc Unverzagt<sup>1,a</sup> for the A2-Collaboration

<sup>1</sup> *Institut für Kernphysik, Johannes Gutenberg-University Mainz, D-55099 Mainz, Germany*

**Abstract.** The Crystal Ball/TAPS setup at MAMI is ideally suited to detect neutral and electromagnetic decays of the  $\eta$  and  $\eta'$  mesons. In this contribution recent results on  $\eta$  and  $\eta'$  decays from the Crystal Ball/TAPS experiment at MAMI are presented. These are the accurate measurement of  $\eta'$  photoproduction cross-sections in the threshold region, the determination of the timelike electromagnetic transition form factors, and a test of low-energy QCD with the  $\eta \rightarrow \pi^0\gamma\gamma$  decay. Finally, further perspectives are discussed.

### 1 Introduction

Studying the decays of the  $\eta$  and  $\eta'$  mesons provides unique information on a variety of physics topics, see [1]. Neutral decays such as the isospin-breaking  $\eta/\eta' \rightarrow 3\pi$  decays are important tests for low-energy Quantum Chromo Dynamics (QCD) and especially Chiral Perturbation Theory ( $\chi$ PT). Another test of  $\chi$ PT is the  $\eta \rightarrow \pi^0\gamma\gamma$  decay which occurs only from order  $O(p^6)$  though low-energy coefficients have to be determined from other models, e.g. Vector Meson Dominance (VMD).

Another important aspect that can be studied with  $\eta$  and  $\eta'$  decays are electromagnetic transition form factors (TFFs) which can be studied through the  $\eta/\eta' \rightarrow e^+e^-\gamma$  Dalitz decays, see also various other contributions to this conference. The TFFs are interesting themselves as they probe the electromagnetic structure of the mesons. They may also give important input to the calculations of the hadronic light-by-light contributions to the anomalous magnetic moment of the muon  $a_\mu = (g-2)_\mu$ . The anomalous magnetic moment  $a_\mu$  is one of the most accurately determined quantities, both from an experimental and theoretical side within the Standard Model (SM). Currently a discrepancy of  $3-4\sigma$  exists between experiment and theory indicating physics beyond the SM.

Here photoproduction cross sections of the  $\eta$  and of the  $\eta'$  in the threshold region measured with the Crystal Ball/TAPS setup at the Mainz Microtron (MAMI) are shown with unprecedented accuracy. Furthermore, studies of timelike transition form factors in  $\eta$  and  $\eta'$  Dalitz decays, and a test of  $\chi$ PT at  $O(p^6)$  and other models through the  $\eta \rightarrow \pi^0\gamma\gamma$  decay are discussed. Before summarising a short outlook on the forthcoming  $\eta/\eta'$  programme with the Crystal Ball/TAPS setup at MAMI will be given. Other interesting topics that can be studied with  $\eta$  and  $\eta'$  decays as the search for violation of lepton-family numbers, placing limits on the masses and couplings of many proposed lepto-quark families [2–6], and investigating violations of

$C$ ,  $CP$ , and  $CPT$  invariance [7] will not be covered by this contribution.

### 2 Experimental Setup

The Crystal Ball/TAPS setup was located at the Institute for Nuclear Physics at the Johannes Gutenberg-University in Mainz, Germany. There three major experiments were installed using the electron beam from the Mainz Microtron (MAMI) accelerator. The results of the A2 collaboration presented here were extracted from data taken with the Crystal Ball/TAPS setup at the Bremsstrahlung facility at MAMI. The A1-setup consisted of four high-resolution spectrometers for electron scattering experiments. The A4-experiment, a high-rate calorimetric detector for the measurement of parity violation in elastic  $ep$ -scattering, was finished in 2012. In 2013 the first steps for installing a new high-luminosity electron accelerator, Mainz Energy-Recovering Superconducting Accelerator (MESA), in the A4-halls were made. Key experiments with MESA, which was funded by the excellence initiative PRISMA [8], were a high-precision measurement of the electro-weak mixing angle in the low energy region, and the search for the Dark Photon. These two experiments and many others performed with MAMI were funded through the Collaborative Research Center 1044 (CRC1044) [9].

MAMI was an electron accelerator consisting of three Race-Track-Microtrons (RTM) [10] and a Harmonic-Double-Sided Microtron (HDSM) [11]. The exceptionally stable beam (energy drift  $\delta E < 100$  keV) could be produced with a maximum energy of  $E_0 = 1604$  MeV and an energy width of  $\sigma_e/E < 3 \cdot 10^{-5}$ . The beam could be delivered with high currents of up to  $110\mu\text{A}$  and high degrees of polarisation of up to 80 %. The operation time of MAMI of about 7000 h per year shows on the one hand its high reliability, and on the other a high interest in hadron physics experiments at MAMI.

The A2 collaboration performed experiments with a real-photon beam (flux  $2.5 \cdot 10^5(\text{sMeV})^{-1}$ ) derived from

<sup>a</sup>e-mail: unvemarc@kph.uni-mainz.de

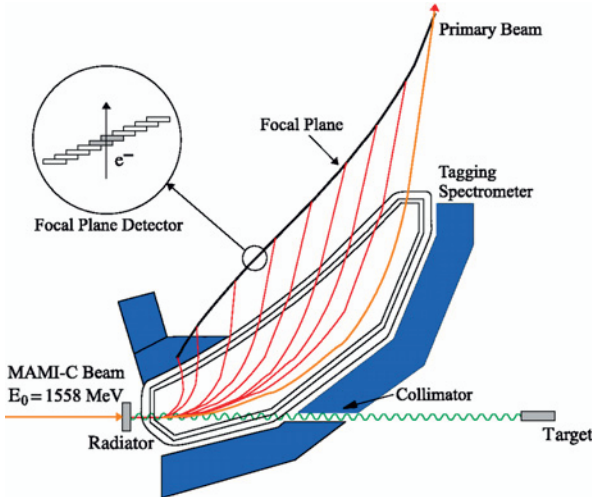


**Figure 1.** The Glasgow-Mainz photon tagging spectrometer at MAMI. From the incoming electron beam from MAMI photons are produced through Bremsstrahlung in a thin radiator foil. Post-radiation electrons are momentum analysed, and thus the photons tagged in energy.

the production of Bremsstrahlung photons during the passage of the MAMI electrons through a thin radiator foil. In the Glasgow-Mainz tagging spectrometer [12–14] post-radiation electrons were momentum analysed in a magnetic field, see fig. 1. From this the post-radiation electron energies  $E_e$  were derived. Thus, the energy of the beam-photons were tagged through  $E_\gamma = E_0 - E_e$  with an energy resolution between 2 to 4 MeV, depending on the incident electron beam energy. Photons could be tagged in the energy range from 5 to 94 % of the incoming electron beam energy. Thus, the highest tagged photon energy for  $E_0 = 1604$  MeV is  $E_\gamma \approx 1492$  MeV.

This maximum tagged photon energy allowed the measurement of only a small part of the  $\eta'$  production range accessible at MAMI. Thus, a new tagging spectrometer, Endpoint tagger (EPT), was constructed to cover the range from  $E_\gamma = 1425$  MeV to  $E_\gamma = 1575$  MeV which was almost the full  $\eta'$  photoproduction range at MAMI. The EPT was based on the same working principle as the main tagging spectrometer, with an energy resolution of approximately 1 MeV.

The central apparatus in the A2-setup was the Crystal Ball detector (CB), see fig. 2, in whose centre a liquid hydrogen target was placed for  $\eta$  and  $\eta'$  production experiments. The Crystal Ball was a self-triggering spectrometer, highly segmented with 672 NaI(Tl) crystals. Each crystal was a 40 cm (15.7 radiation lengths) long truncated triangular pyramid, read out by individual photomultipliers. The CB had an energy resolution of  $\Delta E/E = 0.020(E[\text{GeV}])^{0.36}$ , angular resolutions  $\sigma_\theta$  of 2 – 3° and  $\sigma_\phi$  of  $\sigma_\theta/\sin\theta$  for electromagnetic showers. For charged particle identification the target was surrounded by a barrel detector (PID) made of 24 scintillator strips (50 mm length, 4 mm thickness at a radius of 1 cm around the photon beam line). Energies measured with the PID in com-

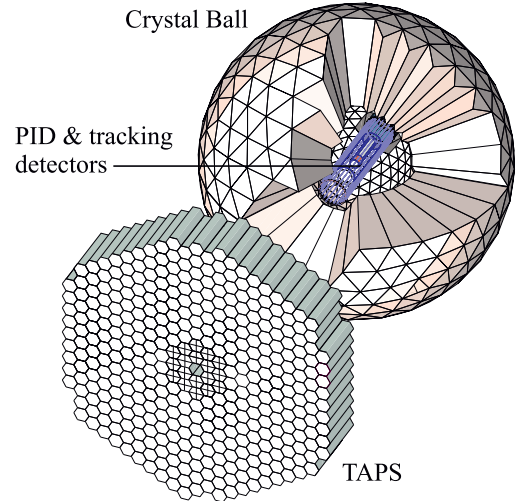


**Figure 2.** The Crystal Ball/TAPS detector setup. The spherical Crystal Ball detector can be seen with cut-away section, showing the inner detectors, and the TAPS forward wall.

bination with energies measured with the CB provided information on the particle type through the  $\Delta E/E$  method.

The CB detector had a forward opening between polar angles  $< 21^\circ$ . This region of the solid angle was covered by the TAPS detector [15, 16]. Thus, the full detector setup, shown in figure 2, was almost hermetic. The TAPS forward wall was composed of two rings of 72  $\text{PbWO}_4$  and several rings of  $\text{BaF}_2$  crystals. The 25 cm (12 radiation lengths) long  $\text{BaF}_2$  crystal had a hexagonal cross section with a diameter of 59 mm. Four  $\text{PbWO}_4$  crystal formed the shape of one  $\text{BaF}_2$  crystal, and had an length of 20 cm (22 radiation length). Each  $\text{BaF}_2$  crystal and each block of four  $\text{PbWO}_4$  crystals had an individual 5 mm thick plastic veto scintillator in front, for charged particle discrimination. The single TAPS counter resolution was 0.2 ns, and the energy resolution can be described by  $\Delta E/E = 0.018 + 0.008/(E[\text{GeV}])^{0.5}$ . The energy resolution of  $\text{PbWO}_4$  crystals for photons is similar to  $\text{BaF}_2$  at room temperature [17], but the higher granularity improves the rate capability and the angular resolution.

### 3 $\eta$ and $\eta'$ Cross Sections

The Crystal Ball/TAPS at MAMI setup was ideal to study the photoproduction of  $\eta$  mesons. The integrated total  $\eta$ -photoproduction cross section reaches almost 100 % already at photon energies of  $E_\gamma = 1400$  MeV. Thus, a further increase in beam energy does not increase the statistical accuracy greatly. Instead new background channels complicate the analysis. Furthermore, the Crystal Ball detector has proven to be ideal for measuring multi-photon final states such as the  $\eta \rightarrow 3\pi^0$  decay.

With the Crystal Ball/TAPS setup a new determination of the  $\eta$ -photoproduction cross sections was performed [18]. The data obtained between the production threshold of  $E_\gamma = 707$  MeV and  $E_\gamma = 1402$  MeV showed unprecedented accuracy. Differential cross sections were

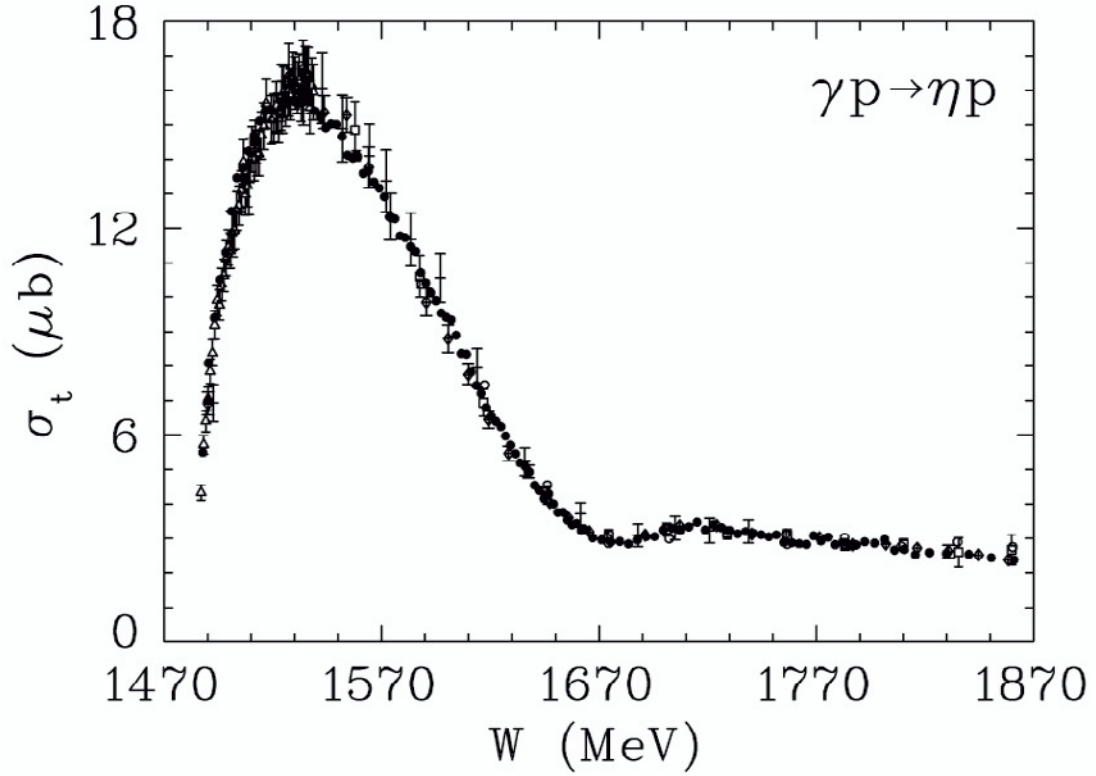


**Figure 3.** Total cross section for  $\gamma p \rightarrow \eta p$  as a function of the c.m. energy from the Crystal Ball/TAPS experiment at MAMI-C [18] (solid circles). The hardly visible uncertainties are of statistical nature only. Other determinations shown for comparison are from MAMI-B [19] (open triangles); CLAS-g1c [20] (open circles); CLAS-g11a [21] (open diamonds); GRAAL [22] (open diamonds with crosses); LNS [23] (horizontal bars); CB-ELSA [24] (open squares); CBELSA/TAPS [25] (crosses).

extracted for the full angular range in the c.m. frame, using  $3.8 \cdot 10^6 \gamma p \rightarrow \eta p \rightarrow 3\pi^0 p \rightarrow 6\gamma p$  accumulated events. This allowed the most precise binning in energy and angle, enabling the reaction dynamics to be studied in greater detail than previously possible. The Crystal Ball/TAPS data agreed very well with previous equivalent measurements, but are remarkably superior in terms of precision and energy resolution [18].

These differential cross sections were integrated to derive the total  $\eta$ -photoproduction cross section shown in figure 3 in comparison to previous measurements [19–25]. As can be seen clearly from the binning of the new Crystal Ball/TAPS at MAMI-C data the statistics are unprecedented. These data have been included in a new SAID partial wave analysis [26] and the Reggeized  $\eta$ -MAID partial wave analysis [27], and have proven to be a substantial contribution.

Recently, first preliminary  $\eta'$ -photoproduction cross sections have been determined with the Crystal Ball/TAPS setup at MAMI-C. Differential cross sections for the range of  $E_\gamma = 1450$  MeV to  $E_\gamma = 1570$  MeV have been obtained with very high accuracy from  $\eta' \rightarrow \eta\pi^0\pi^0 \rightarrow 6\gamma$  decays. This is also reflected in the total  $\eta'$ -photoproduction cross section shown in figure 4, where the Crystal Ball data are compared to results from CBELSA/TAPS. Though the data from Crystal/TAPS are limited in the photon-energy range they show the very high accuracy in the threshold re-

gion already achieved at MAMI-C with a first preliminary  $\eta'$  production run.

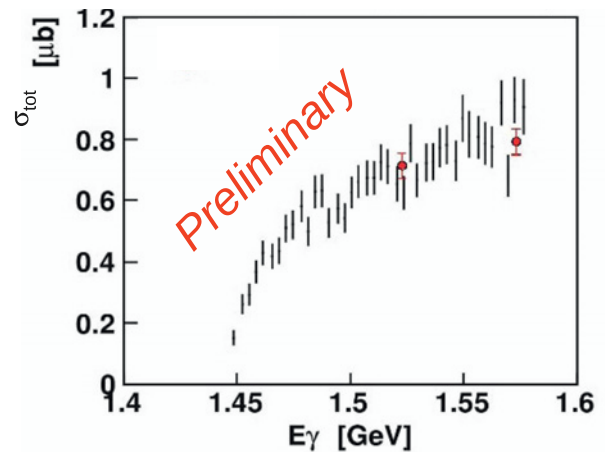


**Figure 4.** Preliminary total cross section for  $\gamma p \rightarrow \eta' p$  from the Crystal Ball/TAPS experiment at MAMI-C (black error bars). Uncertainties are of statistical nature only. These data are compared to CBELSA/TAPS results [25]

## 4 Timelike Transition Form Factors from $\eta/\eta' \rightarrow e^+e^-\gamma$

Electromagnetic transition form factors (TFF) of light pseudoscalar mesons are important for the understanding of the intrinsic structure of these particles (see e.g. [28] and references therein). These TFFs are crucial tests for models describing the structure, e.g. Vector Meson Dominance (VMD) model, and provide for the  $\eta$  and  $\eta'$  mesons information on the mixing of these two particles. Furthermore, it has been argued that TFFs might be related to the hadronic light-by-light contribution to the anomalous magnetic moment of the muon [29]. Thus, it is of great importance to test the TFFs at as high a precision as possible.

The TFF for the  $\eta$  meson can be studied in the timelike momentum transfer region through the  $\eta \rightarrow \gamma^*\gamma \rightarrow e^+e^-\gamma$  decay with the Crystal Ball/TAPS setup. A first determination from the A2 collaboration based on  $1.35 \cdot 10^3$   $\eta \rightarrow e^+e^-\gamma$  decays, extracted using kinematic cuts, was published in 2011 [30]. The result can be seen in figure 5 in comparison to earlier measurements. The SND collaboration also used the  $\eta \rightarrow e^+e^-\gamma$  decay with significantly lower statistics [31] than from the Crystal Ball/TAPS measurement. The measurement of the NA60 collaboration [32] with  $9 \cdot 10^3$   $\eta \rightarrow \mu^+\mu^-\gamma$  decays had the highest precision up to that date though this result has two major shortcomings. Due to the decay into muons the distribution only starts at  $q = 2m_\mu$ , and only the leptons were detected in their setup. All results are in good agreement, and also match the theoretical calculation of Terschlußen and Leupold [33] based on a vector-meson Lagrangian combined with the Wess-Zumino-Witten contact interaction.

Recently, the A2 collaboration has determined a new preliminary result for the  $\eta$  TFF measured with the Crystal Ball/TAPS setup. This new analysis was based on the kinematic fitting technique and used a bigger data set three times larger than for the previous A2 determination. Also due to the kinematic fitting technique the full  $\eta$ -photoproduction range accessible at MAMI could be explored. This resulted in  $18 \cdot 10^3$  analysed  $\eta \rightarrow e^+e^-\gamma$  decays, more than one order of magnitude better statistics. If the detection of the outgoing proton from the  $\gamma p \rightarrow \eta p$  reaction was not required the statistics could be increased to  $22 \cdot 10^3$  decays but with poorer signal-to-background ratio.

Figure 6 shows the preliminary results of this new analysis. A fit of the usual one-pole approximation to the data points was done. Perfect agreement with the old A2 measurement [30] and the NA60 [32] results can be seen as well as comparisons to three theoretical calculations. The new A2 result clearly surpasses the published NA60 accuracy, although a preliminary determination from NA60 [34] has been presented with  $80 \cdot 10^3$   $\eta \rightarrow \mu^+\mu^-\gamma$  decays from a new measurement. All theoretical calculations in figure 6 describe the A2 data points within the uncertainties. The calculation by Terschlußen and Leupold [33], which combines the vector-meson Lagrangian proposed in ref. [35], and recently extended in ref. [36], with the Wess-Zumino-Witten contact interaction, runs below the fit to the A2 data points. The model-

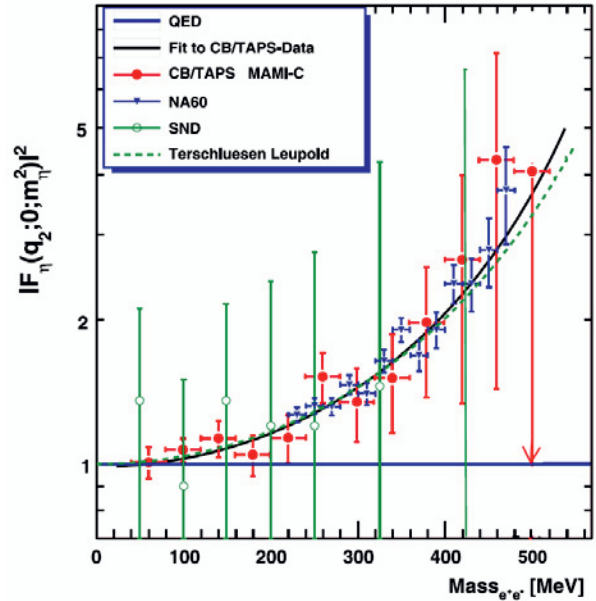


**Figure 5.** First result on the  $\eta$  TFF from the Crystal Ball/TAPS setup [30] (red full circles). Data are compared to experimental results of the SND [31] (green open circles) and NA60 [32] (blue triangles) collaborations. The dashed green line is a theoretical calculation [33] based on a vector-meson Lagrangian combined with the Wess-Zumino-Witten contact interaction.

independent method using Padé-approximants that was developed for the  $\pi^0$  TFF in ref. [37] uses spacelike data to provide a model-independent prediction for the timelike TFF [38]. This calculation almost perfectly agrees with the fit. The calculation by the Jülich group establishes a connection between the radiative  $\eta \rightarrow \pi^+\pi^-\gamma$  and the isovector contributions to the  $\eta \rightarrow \gamma^*\gamma$  TFF using dispersion theory. The resulting curve from this calculation lies slightly above the fit to the A2 data. The inability to distinguish between these models clearly calls for higher precision measurements of the  $\eta$  TFF.

For the determination of the  $\eta'$  TFF from  $\eta' \rightarrow e^+e^-\gamma$  decays first studies were done for 20 background channels [40]. Based on these results up to 80  $\eta \rightarrow e^+e^-\gamma$  events might be extracted from the 5-week  $\eta'$  production data taken in 2012. In summer 2014 new  $\eta'$  data will be taken with up to a factor 10 higher statistics. Thus far no result for the  $\eta' \rightarrow e^+e^-\gamma$  decay has been published, though other experiments, e.g. CLAS and BESIII, are capable of measuring the  $\eta'$  TFF too. The new A2 measurement will enable one of the most accurate determinations for the  $\eta'$  transition form factor.

## 5 Preliminary Results for $\eta \rightarrow \pi^0\gamma\gamma$

The major contribution to the  $\eta \rightarrow \pi^0\gamma\gamma$  decay amplitude stems from  $O(p^6)$  counterterms. These are needed in  $\chi$ PT to cancel divergences. Lower order terms do not contribute because they are forbidden or largely suppressed. Studying this decay is not a strict test of  $\chi$ PT but rather of the models used to calculate the low-energy coefficients of the coun-

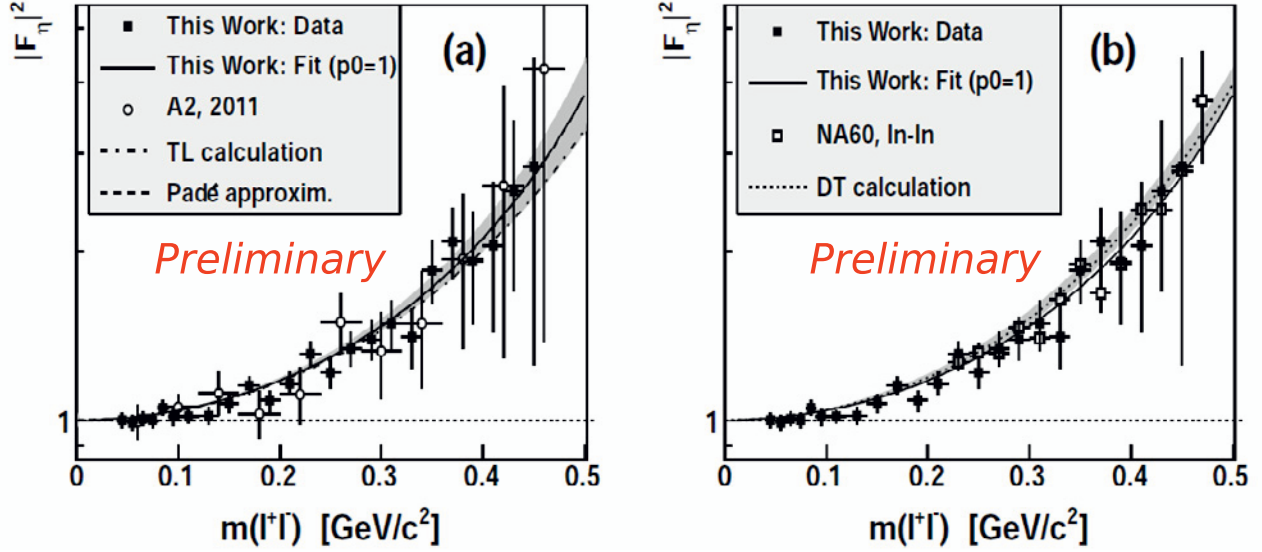


**Figure 6.** New result on the  $\eta$  TFF from the Crystal Ball/TAPS setup (full squares). Data are compared in (a) to the first A2 determination [30] (open circles) and in (b) to the result from the NA60 collaboration [32] (open squares). Theoretical calculations are in (a) from Terschläusen and Leupold (TL) [33] (dashed-dotted line) and the model independent method based on Padé-approximants [38] (dashed line with error band). In (b) a calculation based on dispersion theory (DT) is shown [39] (dotted line with error band).

terterms that can not be determined with  $\chi$ PT itself. All calculations must describe the decay width  $\Gamma(\eta \rightarrow \pi^0\gamma\gamma)$  as well as the differential decay rate  $d\Gamma/dm^2(\gamma\gamma)$ . But for the two quantities discrepancies existed between models for  $d\Gamma/dm^2(\gamma\gamma)$  and between experimental results for  $\Gamma(\eta \rightarrow \pi^0\gamma\gamma)$ , respectively.

A new analysis of data taken with the Crystal Ball/TAPS setup using kinematic fitting yielded  $1.2 \cdot 10^3$   $\eta \rightarrow \pi^0\gamma\gamma$  events. The preliminary result for the differential decay rate is shown in figure 7. Only three other experimental studies are known up to now. A preliminary analysis of earlier Crystal Ball/TAPS data [41] yielded only around 150  $\eta \rightarrow \pi^0\gamma\gamma$  events but the old and the new Crystal Ball/TAPS results agree within the uncertainties. The Crystal Ball at AGS result from 2008 [42] with roughly 500 events had much better statistics than the old Crystal Ball/TAPS measurement though with a poorer signal-to-background ratio. A third determination was carried out by the WASA at COSY collaboration [43] but was not published in a journal yet. The data show general agreement with the Crystal Ball/TAPS results and a similar accuracy, though only statistical errors are provided. Thus, the new Crystal Ball/TAPS analysis provides the most accurate result with the best signal-to-background ratio to date.

In figure 7 three theoretical calculations are compared with the experimental results: a calculation based on the VMD transition amplitude [44], a revised calculation of this based on a chiral unitary approach [45], and a calculation involving theoretical studies of photon fusion reactions based on a chiral Lagrangian with dynamical light vector mesons [46]. All three theoretical studies agree within the uncertainties with the experimental results. Thus, more detailed measurements are needed to distinguish between the models and also to perform a Dalitz-plot analysis of the  $\eta \rightarrow \pi^0\gamma\gamma$  decay.

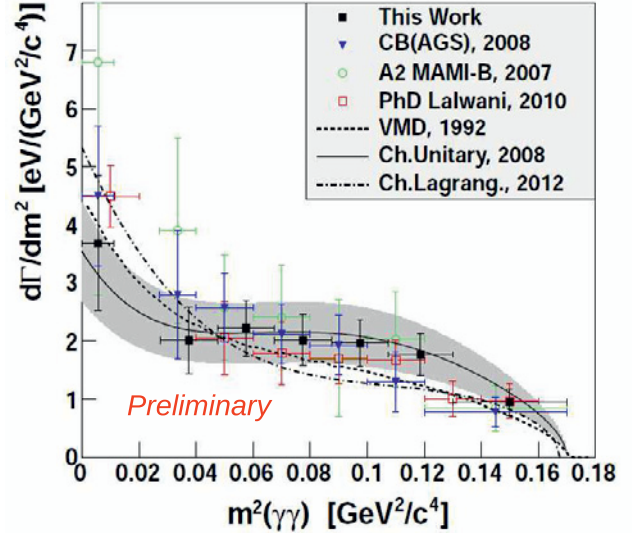


**Figure 7.** Preliminary differential decay rate for  $\eta \rightarrow \pi^0\gamma\gamma$  measured with the Crystal Ball/TAPS setup. For comparison previous results from the A2 collaboration [41] (green circles), the Crystal Ball at AGS [42] (blue triangles), and the WASA at COSY collaboration [43] (red open squares) are shown. Also theoretical calculations using VMD transition amplitudes [44] (dashed line), based on a chiral unitary approach [45] (solid line with error band), and based on a chiral Lagrangian with dynamical light vector mesons [46] (dash-dotted line) are visible.

The preliminary value from the new Crystal Ball/TAPS analysis for the decay width,  $\Gamma(\eta \rightarrow \pi^0\gamma\gamma) = (0.33 \pm 0.03_{tot})$  eV, agrees very well with all recent experimental and theoretical results. Earlier measurements showed both large discrepancies and uncertainties. The new Crys-

tal Ball/TAPS determination of the decay width is the most accurate value to date.

## 6 Future Programme at MAMI

The programme on  $\eta/\eta'$  physics in the A2 collaboration will be continued in summer 2014 with the installation of the End-point tagger and several weeks of  $\eta'$ -photoproduction. Compared to the 2012 data taking the speed of the data acquisition system will be increased at least by a factor 4. It is planned to measure enough statistics to reach the goals of  $4 \cdot 10^5$  analysed  $\eta' \rightarrow \eta\pi^0\pi^0$  (to perform a Dalitz plot analysis) and roughly 800 analysed  $\eta' \rightarrow e^+e^-\gamma$  decays for the determination of the TFF. The statistics on the  $\eta \rightarrow \pi^0\gamma\gamma$  decay will be improved significantly to perform a first Dalitz-plot analysis.

The long-term plans foresee the improvement of the knowledge on TFFs extracted from single and double Dalitz-decays. Also the possibility of studying the TFF in the  $\omega \rightarrow \pi^0e^+e^-$  decay will be explored. Furthermore, Dalitz-plot analyses of the  $\eta/\eta' \rightarrow 3\pi^0$  and the  $\eta' \rightarrow \eta\pi^0\pi^0$  decays will be carried out. In the latter decay also the cusp effect will be studied. Another possibility is to investigate radiative decays like  $\eta' \rightarrow \omega\gamma$  and  $\omega \rightarrow \pi^0/\eta\gamma$ . In the even further planning an improved tracking is planned to also measure several charged decays of the  $\eta$  and  $\eta'$  mesons with high accuracy.

## 7 Summary

In this contribution several new results from the A2 collaboration on  $\eta$  and  $\eta'$  physics were presented. The Crystal Ball/TAPS setup has proven to be ideal for the measurement of many neutral and leptonic decays of the  $\eta$  and  $\eta'$  mesons, producing world-leading results. Here total cross sections for  $\eta$ - and preliminary total cross sections for  $\eta'$ -photoproduction were described which show unprecedented accuracy, especially in the threshold regions. Furthermore, two determinations of the electromagnetic transition form factor from  $\eta \rightarrow e^+e^-\gamma$  decays were shown. The latest A2 result is currently the most precise determination. First studies of the  $\eta'$  transition form factor were also presented. Finally, the partial decay rate and the decay width of the  $\eta \rightarrow \pi^0\gamma\gamma$  decay with the world's best precision to date were demonstrated. In future results on the above mentioned determinations will be improved greatly and further neutral and leptonic decays will be studied with high accuracy.

## References

- [1] J. Bijnens, G. Fäldt, and B.M.K. Nefkens (Editors), Phys. Scripta T **99** (2002).
- [2] J.L. Goity, A.M. Bernstein, and B.R. Holstein, Phys. Rev. D **66**, 076014 (2002).
- [3] M.J. Ramsey-Musolf and M.B. Wise, Phys. Rev. Lett. **89**, 041601 (2002).
- [4] B.V. Martemyanov and V.S. Sopov, Phys. Rev. D **71**, 017501 (2005).
- [5] A.G. Nicola and J.R. Pelaez, Phys. Rev. D **65**, 054009 (2002).
- [6] P. Herczeg, Phys. Rev. D **51**, 136 (1995).
- [7] B.M.K. Nefkens, Few-Body Syst. Suppl. **9**, 193 (1995).
- [8] <http://www.prisma.uni-mainz.de> (14th December 2013).
- [9] <http://sfb1044.kph.uni-mainz.de/sfb1044/> (14th December 2013).
- [10] H. Herminghaus *et al.*, IEEE Trans Nucl. Sci. **30**, 3274 (1983).
- [11] K.-H. Kaiser *et al.*, Nucl. Instrum. Meth. A **593**, 159 (2008).
- [12] I. Anthony *et al.*, Nucl. Instr. Meth. A **310**, 230 (1991).
- [13] S.J. Hall [*et al.*], Nucl. Instr. Meth. A **368**, 698 (1996).
- [14] J.C. McGeorge *et al.*, Eur. Phys. J. A **37**, 129 (2008).
- [15] R. Novotny, IEEE Trans. Nucl. Sci. **38**, 379 (1991).
- [16] A.R. Gabler *et al.*, Nucl. Instrum. Meth. **A346**, 168 (1994).
- [17] R. Novotny *et al.*, Nucl. Instrum. Meth. A **486**, 131 (2002).
- [18] E.F. McNicoll *et al.*, Phys. Rev. C **82**, 035208 (2010).
- [19] B. Krusche *et al.*, Phys. Rev. Lett. **74**, 3736 (1995).
- [20] M. Dugger *et al.* (CLAS Collaboration), Phys. Rev. Lett. **89**, 222002 (2002).
- [21] M. Williams *et al.* (CLAS Collaboration), Phys. Rev. C **80**, 045213 (2009).
- [22] O. Bartalini *et al.* (GRAAL Collaboration), Eur. Phys. J. A **33**, 169 (2007).
- [23] T. Nakabayashi *et al.*, Phys. Rev. C **74**, 035202 (2006).
- [24] V. Créde *et al.* (CB-ELSA Collaboration), Phys. Rev. Lett. **94**, 012004 (2005).
- [25] V. Créde *et al.* (CB-ELSA/TAPS Collaboration), Phys. Rev. C **80**, 055202 (2009).
- [26] W.J. Briscoe, D. Schott, I.I. Strakovsky, and R.L. Workman, <http://gwdac.phys.gwu.edu>.
- [27] W.-T. Chiang, S.-N. Yang, L. Tiator, M. Vanderhaeghen, and D. Drechsel, Phys. Rev. C **68**, 045202 (2003).
- [28] E. Czerwinski, S. Eidelman, C. Hanhart, B. Kubis, A. Kupść, S. Leupold, P. Moskal, and S. Schadmand (Editors), Proceedings of *First MesonNet Workshop on Meson Transition Form Factors*, 2012, Cracow, Poland, arXiv:1207.6556 [hep-ex].
- [29] F. Jegerlehner and A. Nyffeler, Phys. Rep. **477**, 1 (2009).
- [30] H. Berghäuser *et al.*, Phys. Lett. B **701**, 562 (2011).
- [31] M.N. Achasov *et al.*, Phys. Lett. B **504**, 275 (2001).
- [32] R. Araldi *et al.*, Phys. Lett. B **677**, 260 (2009).
- [33] C. Terschlüsen, Diploma thesis, University Gießen, Germany, 2010.
- [34] A. Uras for the NA60 collaboration, Acta Phys. Pol. B **5**, 465 (2012).
- [35] M.F.M. Lutz and S. Leupold, Nucl. Phys. A **813**, 96 (2008).

- [36] C. Terschläsen, S. Leupold, and M.F.M. Lutz, Eur. Phys. J. A **48**, 190 (2012).
- [37] P. Masjuan, Phys. Rev. D **86**, 094021 (2012).
- [38] R. Escribano, P. Masjuan, and P. Sanchez-Puertas, arXiv:1307.2061 [hep-ph].  
P. Masjuan and P. Sanchez-Puertas, Johannes Gutenberg-University Mainz, Germany, private communication, 2013.
- [39] C. Hanhart, A. Kupść, U.-G. Meißner, F. Stollenwerk, and A. Wirzba, arXiv:1307.5654 [hep-ph].  
C. Hanhart, Forschungszentrum Jülich, Germany, private communication, 2013.
- [40] S. Wagner, Master thesis, Johannes Gutenberg-University Mainz, Germany, 2013.
- [41] S. Prakhov, Proceedings of MENU 2007, published in eConf C070910, 159 (2007).
- [42] S. Prakhov *et al.*, Phys. Rev. C **78**, 015206 (2008).
- [43] K. Lalwani, Ph.D. thesis, Department of Physics, Indian Institute of Technology, Bombay, India, 2010.
- [44] J.N. Ng and D.J. Peters, Phys. Rev. D **46**, 5034 (1992).
- [45] E. Oset, J.R. Peláez, and L. Roca, Phys. Rev. D **77**, 073001 (2008).
- [46] I.V. Danilkin, M.F.M. Lutz, S. Leupold, and C. Terschläsen, arXiv:1211.1503 [hep-ph].